CORRECTED 16 OCTOBER 2017; SEE FULL TEXT

APPLIED SCIENCES AND ENGINEERING

Rapid and near-complete dissolution of wood lignin at ≤80°C by a recyclable acid hydrotrope

Liheng Chen,[1,2] Jinze Dou,[3] Qianli Ma,[2,4] Ning Li,[5] Ruchun Wu,[2,6] Huiyang Bian,[2,7] Daniel J. Yelle,[2] Tapani Vuorinen,[3] Shiyu Fu,[4] Xuejun Pan,[5] Junyong (J.Y.) Zhu[2,5]*

We report the discovery of the hydrotropic properties of a recyclable aromatic acid, *p*-toluenesulfonic acid (*p*-TsOH), for potentially low-cost and efficient fractionation of wood through rapid and near-complete dissolution of lignin. Approximately 90% of poplar wood (NE222) lignin can be dissolved at 80°C in 20 min. Equivalent delignification using known hydrotropes, such as aromatic salts, can be achieved only at 150°C or higher for more than 10 hours or at 150°C for 2 hours with alkaline pulping. *p*-TsOH fractionated wood into two fractions: (i) a primarily cellulose-rich water-insoluble solid fraction that can be used for the production of high-value building blocks, such as dissolving pulp fibers, lignocellulosic nanomaterials, and/or sugars through subsequent enzymatic hydrolysis; and (ii) a spent acid liquor stream containing mainly dissolved lignin that can be easily precipitated as lignin nanoparticles by diluting the spent acid liquor to below the minimal hydrotrope concentration. Our nuclear magnetic resonance analyses of the dissolved lignin revealed that *p*-TsOH can depolymerize lignin via ether bond cleavage and can separate carbohydrate-free lignin from the wood. *p*-TsOH has a relatively low water solubility, which can facilitate efficient recovery using commercially proven crystallization technology by cooling the concentrated spent acid solution to ambient temperatures to achieve environmental sustainability through recycling of *p*-TsOH.

INTRODUCTION

Economical and sustainable deconstruction or fractionation of lignocellulose cell walls into usable building blocks or platform molecules is key to achieving a green biobased economy (*1*). A variety of fractionation technologies have been developed to address this issue, such as dilute acid (*2*), alkaline (*3*), organosolv (*4*–*6*), ionic liquid (*7*), and sulfite (*8*, *9*), but all with limited commercial success. Delignification is critical for successful cell wall deconstruction because lignin is a major cell wall polymer, with the middle lamella lignin acting as a glue to hold cells together in plant biomass (*10*). Furthermore, lignin has the potential to develop a variety of bioproducts (*11*–*13*). However, delignification processes are energy-intensive, which is a well-known challenge in the pulp and paper industry. Existing delignification technologies, such as alkaline and sulfite pulping processes, all need to be operated at high temperatures, use pressurized vessels, and have costly chemical recovery. Therefore, we need to develop low-temperature and rapid delignification with simplistic recovery of chemicals for advanced utilization of renewable and biodegradable lignocelluloses for the future biobased economy.

Here, we report the discovery of an aromatic acid, *p*-toluenesulfonic acid (*p*-TsOH), as a hydrotrope for unparalleled performance in delignification at low temperatures below the water boiling point. We were able to dissolve a substantial (approximately 90%) amount of wood lignin at 80°C or lower and within a short 20-min period. Equivalent delignification can be achieved only at 150°C for 2 hours using alkaline wood pulping or at approximately 150°C for more than 10 hours (*14*) using known hydrotropes, such as aromatic salts [at 170°C for 2 hours with catalyst (*15*)]. Certain solvent processes can solubilize cellulose at low temperatures (*16*), thus allowing for a degree of lignin separation, but these processes produce amorphous cellulose that has limited utility and a lignin material with unknown characteristics. Figure 1A schematically shows that we can use this type of acid hydrotrope to fractionate wood into two principal components: (i) a primarily carbohydrate-rich water-insoluble solid (WIS) fraction that can be used to produce lignocellulosic nanomaterials [such as lignocellulose nanofibrils (*17*)], fibers, and/or sugars through (enzymatic) hydrolysis; and (ii) a spent acid liquor stream containing mainly dissolved lignin that can be easily precipitated in the form of lignin nanoparticles (LNPs) by diluting the spent acid liquor to below the minimal hydrotrope concentration (MHC), as schematically shown in Fig. 1B. Because *p*-TsOH has low solubility at ambient temperatures, we can achieve efficient *p*-TsOH recovery using crystallization technology by cooling concentrated spent acid solution to ambient temperatures.

Rapid and near-complete delignification with simplified separation and efficient recovery of used chemicals allows for a low energy input and sustainable production of valuable building blocks, such as sugars, fibers, and wood-based nanomaterials, from renewable and biodegradable resources for the future biobased economy. The unparalleled performance in delignification may also have the potential to develop disruptive technologies for replacing existing pulping technologies developed more than a century ago. Therefore, this study may also have an impact on the existing pulp industry facing energy and environmental issues.

RESULTS AND DISCUSSION

Wood fractionation

We fractionated Wiley-milled poplar NE222 particles using concentrated *p*-TsOH aqueous solutions at varied concentrations, reaction temperatures, and times. We calculated the fraction of a component remaining (*R*) in the washed WIS after fractionation using the yield and

[1]Key Laboratory of Biomaterials of Guangdong Higher Education Institutes, Department of Biomedical Engineering, Jinan University, Guangzhou, China. [2]Forest Products Laboratory, U.S. Department of Agriculture Forest Service, Madison, WI 53726, USA. [3]Department of Bioproducts and Biosystems, School of Chemical Engineering, Aalto University, Espoo, Finland. [4]State Key Laboratory of Pulp and Paper Engineering, South China University of Technology, Guangzhou, China. [5]Department of Biological Systems Engineering, University of Wisconsin-Madison, Madison, WI 53706, USA. [6]School of Chemistry and Chemical Engineering, Guangxi University for Nationalities, 188 Daxue East Road, Xixiangtang District, Nanning, China. [7]Jiangsu Co-Innovation Center of Efficient Processing and Utilization of Forest Resources, Nanjing Forestry University, Nanjing, China.
*Corresponding author. Email: jzhu@fs.fed.us

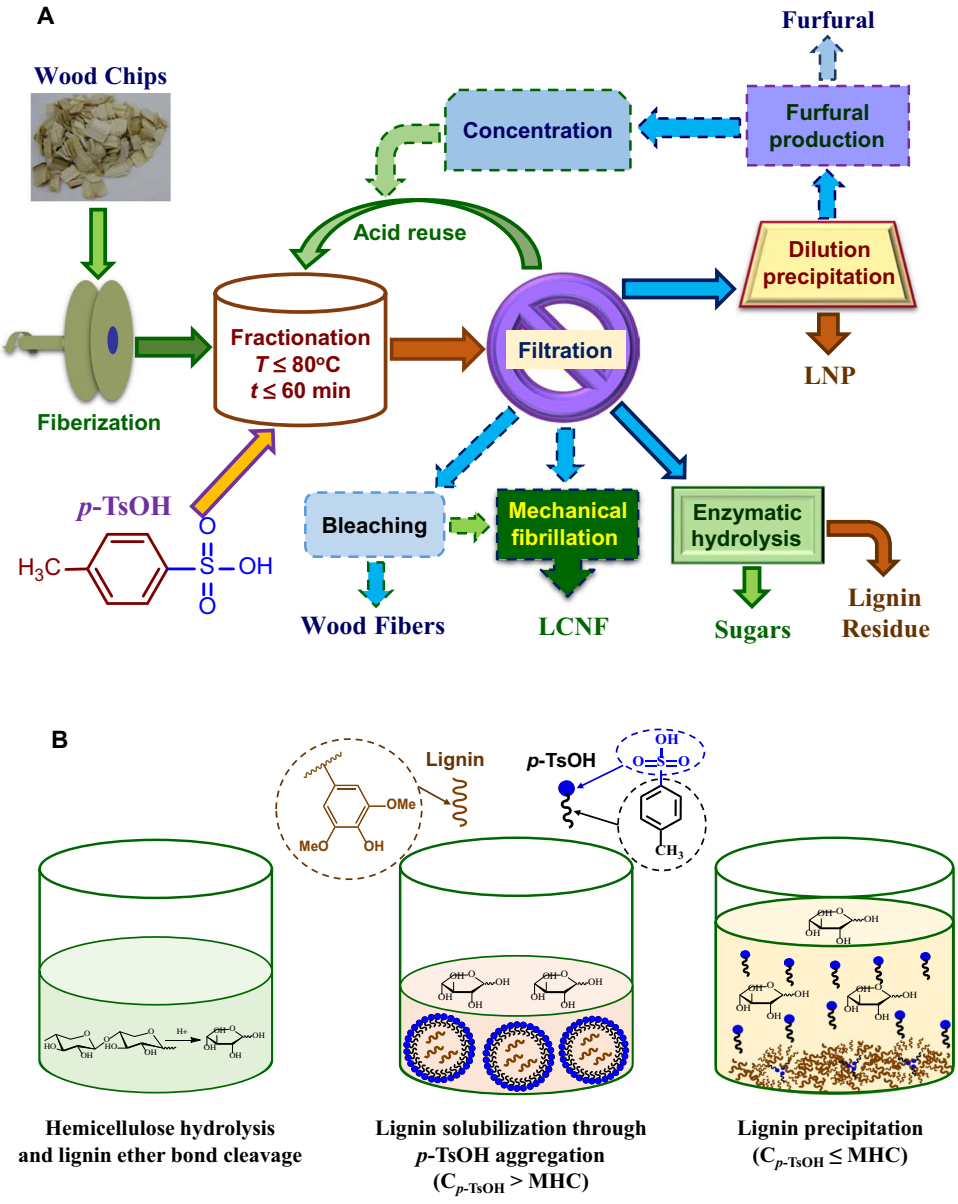

Fig. 1. Description of the present wood fractionation experimental study and lignin solubilization mechanism. (**A**) Schematic flow diagram shows wood fractionation using *p*-TsOH for the production of fibers, lignocellulosic nanomaterials, sugars, and LNPs. Processes with dashed lines were not carried out in this study. (**B**) Schematics of carbohydrate and lignin solubilization by *p*-TsOH ($C_{p\text{-TsOH}}$ > MHC) and precipitation ($C_{p\text{-TsOH}}$ ≤ MHC).

chemical composition of WIS based on the component in the untreated poplar wood. We were able to solubilize approximately 90% of NE222 (hardwood) lignin at 80°C or lower within 20 min (Fig. 2). We were also able to dissolve approximately 65 to 85% xylan and achieve a minimal glucan loss of approximately 15% or less, especially at a temperature of 65°C or lower. As a result, we fractionated poplar NE222 into a cellulose-rich WIS fraction and a spent acid liquor stream that contains primarily lignin and some hemicelluloses.

We found that increasing the *p*-TsOH concentration can improve lignin solubilization (Fig. 2A) because *p*-TsOH, as a hydrotrope, relies on aggregation to solubilize lignin, as discussed below. We also found that increasing the fractionation temperature can substantially improve both lignin and xylan solubilization (Fig. 2B). However, neither fractionation temperature nor *p*-TsOH concentration affected glucan degradation. We found that reaction time had a minimal effect on lignin and xylan solubilization and glucan degradation except within the first 20 min of reaction under the experimental conditions studied (Fig. 2C). These data indicate a very rapid process for wood fractionation. At high reaction severities [for example, *p*-TsOH concentration P = 80 weight % (wt %) and T = 80°C], longer reaction times over 35 min resulted in increased lignin content in WIS (Fig. 2D), which suggests that solubilized lignin may have been condensed and then reprecipitated. However, xylan dissolution was not much affected at longer reaction times at these high severities. It seems that *p*-TsOH is more selective in solubilizing the five-carbon hemicellulose, such as xylan, than the six-carbon hemicellulose mannan (Fig. 2D).

Table 1. Chemical compositions of *p*-TsOH fractionated poplar NE222 samples under different treatment conditions. The numbers in the parentheses are component yields based on components in the untreated NE222. Numbers indicate what percent of the sum of the integrals for structures Aa and Ca is accounted for by the integral for each individual structure.

Sample label	WISs					Spent liquor				
	Solids yield (%)	Glucan (%)	Xylan (%)	Mannan (%)	Lignin (%)	Glucose (g/liter)	Xylose (g/liter)	Mannose (g/liter)	Acetic acid (g/liter)	Furfural (g/liter)*
Untreated NE222	100	45.7	14.9	4.6	23.4					
P70T50t20	78.9	56.8 (97.9)	8.8 (46.7)	3.3 (56.4)	20.6 (69.4)					
P70T65t20	68.4	61.6 (92.2)	6.5 (29.8)	4.3 (63.9)	11.8 (34.4)					
P70T50t35	74.4	62.2 (101.1)	7.4 (37.0)	4.3 (68.9)	19.2 (61.0)	1.1 (2.2)	8.9 (52.4)	1.0 (20.3)	1.1	0.05 (0.5)
P70T65t35	64.1	68.0 (95.3)	6.6 (28.4)	4.6 (64.0)	13.0 (35.7)	1.3 (2.5)	10.1 (59.5)	1.5 (29.9)	1.5	0.08 (0.7)
P70T80t35	55.5	67.3 (81.7)	4.9 (18.3)	4.2 (50.5)	6.7 (15.8)	1.8 (3.6)	11.6 (68.3)	2.0 (38.7)	1.5	0.19 (1.7)
P70T80t20	58.9	63.0 (81.1)	6.5 (24.5)	4.3 (53.8)	8.8 (22.1)	1.5 (3.0)	11.0 (65.0)	1.8 (35.2)	1.6	0.13 (1.2)
P75T65t05	67.1	56.2 (82.4)	6.5 (29.3)	4.1 (60.0)	15.0 (42.9)	1.2 (2.4)	10.1 (59.7)	1.5 (29.3)	1.5	0.07 (0.6)
P75T65t20	60.7	71.8 (95.4)	5.8 (23.8)	4.9 (63.7)	10.8 (28.0)	1.4 (2.7)	10.8 (64.0)	1.7 (32.4)	1.5	0.10 (0.9)
P75T65t35	59.0	71.7 (94.5)	6.0 (23.9)	4.0 (51.3)	8.9 (22.3)	1.3 (2.6)	10.3 (60.8)	1.7 (32.4)	1.4	0.10 (0.9)
P75T65t60	57.0	74.7 (93.1)	5.0 (19.2)	4.3 (52.8)	7.4 (17.9)	1.7 (3.2)	10.7 (63.4)	1.8 (34.6)	1.5	0.14 (1.2)
P75T80t20	55.0	72.4 (87.1)	5.2 (19.1)	4.4 (52.7)	6.1 (14.4)	1.8 (3.6)	10.9 (64.2)	2.0 (39.7)	1.5	0.19 (1.7)
P80T80t20	51.9	72.3 (81.9)	3.7 (13.0)	3.7 (41.8)	4.2 (9.2)	2.3 (4.6)	9.9 (58.4)	2.2 (43.9)	1.4	0.33 (3.1)
P80T80t35	50.8	75.0 (83.4)	3.6 (12.3)	2.9 (31.7)	4.8 (10.4)					
P80T80t60	57.6	68.2 (85.9)	3.2 (12.4)	2.4 (30.0)	8.3 (20.3)					

*Expressed as a percentage of total lignin content (G + S + S′) in each sample spectrum.

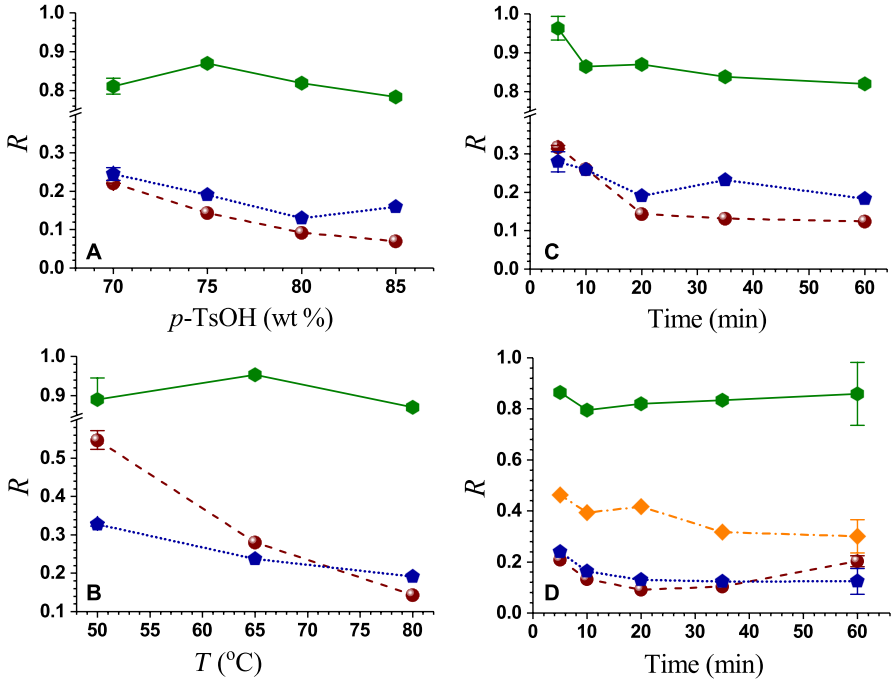

Fig. 2. Effects of reaction conditions on dissolution (1 − *R*) of lignin (●) and carbohydrates (glucan, ⬢; xylan, ⬟; mannan, ◆). *R* is based on the component in untreated poplar wood. (**A**) *p*-TsOH concentration effects for 20 min at 80°C. (**B**) Temperature effects at *p*-TsOH concentration *P* = 75 wt % for 20 min. (**C** and **D**) Time effects at *P* = 75 wt % and 80°C (C) and at *P* = 80 wt % and 80°C (D).

We found that the dissolved carbohydrates in the spent liquor were mainly in the form of monomeric sugars because of the rapid and low-temperature *p*-TsOH fractionation (Table 1). Xylan recovery from the retained xylan and dissolved xylose (not including oligomeric xylose in the spent liquor) was near 90% based on xylan content in untreated poplar NE222. Degradation of xylose to furfural was minimal, which was less than 2% for most runs. Acetic acid concentration in the spent liquor was very low, which was less than 1.5 g/liter. These data suggest *p*-TsOH fractionation can also efficiently recover hemicellulosic sugars.

Separation of dissolved lignin

Most hydrotropes aggregate above MHC (*18*, *19*), or critical aggregate concentration, to solubilize hydrophobic materials. We determined the MHC of *p*-TsOH from the conductivities of its solutions (*20*). We found a transition concentration of 11.5 wt % at which the conductivity of the *p*-TsOH solution shows an abrupt change (Fig. 3A), suggesting that *p*-TsOH starts to lose its hydrotropic properties below the MHC of 11.5 wt %.

We can therefore easily precipitate the dissolved lignin by diluting *p*-TsOH in the spent liquor to below the MHC of 11.5 wt %. As an example, we diluted the spent liquor from Wiley-milled NE222 fractionated at a *p*-TsOH concentration of 75 wt % at 80°C for 20 min (abbreviated as P75T80t20 to simplify discussion) using deionized (DI) water. We monitored the MHC at which lignin precipitation occurred by dynamic light scattering (DLS). The DLS-measured effective lignin particle sizes at different dilutions indicated that lignin precipitation was minimal at *p*-TsOH concentrations greater than 15%, as evidenced by the very small measured particle size of less than 300 nm and the minimal increase in size with dilution from the initial high concentration (Fig. 3B). The measured particle size rapidly increased to approximately 3000 nm when we diluted the spent liquor to 10 wt %. The increase in particle size was not substantial with further dilution to below 4 wt %.

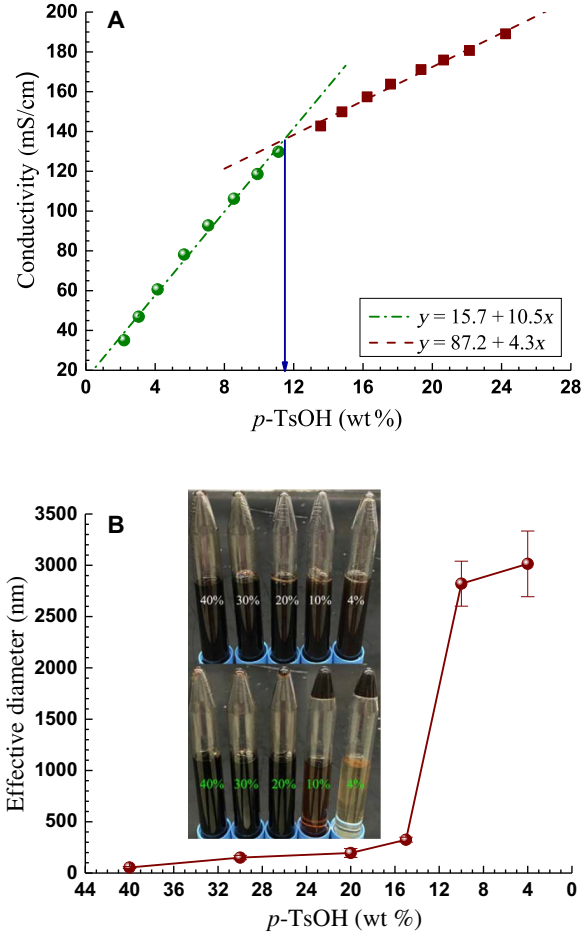

Fig. 3. Determining the *p*-TsOH MHC by (**A**) measuring the conductivities of aqueous *p*-TsOH solutions of different concentrations, showing discontinuity at the *p*-TsOH MHC of 11.5 wt % and by (**B**) measuring the effective size of lignin particles in diluted spent *p*-TsOH liquors using DLS [inset shows images of the diluted spent *p*-TsOH liquor with (bottom) and without (top) centrifugation].

We centrifuged the diluted spent liquor samples at different *p*-TsOH concentrations (top panel of the inset in Fig. 3B) at 3000*g* for 10 min. We observed lignin precipitation from the bottom panel of the inset in Fig. 3B (we placed the centrifuged tubes upside down to separate the precipitates from the supernatant) at a *p*-TsOH concentration of 10 wt % or lower, but it was minimal at 20 wt % or higher. This finding verified the MHC of 11.5 wt % determined from conductivity measurements (Fig. 3A). We found that precipitation increased substantially with further dilution to 4 wt %, and the supernatant changed from highly opaque to clear.

Properties of dissolved lignin

We air-dried the diluted spent liquor at 10 wt % and examined it on a fresh mica by atomic force microscopy (AFM) topographic imaging. The image (Fig. 4A) confirmed that nanoscale lignin particles formed through the self-assembly of dissolved lignin after precipitation through dilution. We observed both aggregated particles (indicated by the multiple peaks in profile 1 in Fig. 4B, corresponding to line 1 in Fig. 4A) and nonaggregated particles [indicated by the separated single peaks in profile 2 (dashed line in Fig. 4B), corresponding to line 2 in Fig. 4A] with diameters between 200 and 800 nm. We found that the lateral sizes of these LNPs ranged from 100 nm to 1.5 μm.

Interest in using LNPs for developing biodegradable materials is growing for many potential applications (*21*–*25*). Reported work on LNP production used commercial alkali lignin that is inexpensive and available in large quantities, but requires dissolving the lignin in solvents, such as ethylene glycol (*26*), acetone, tetrahydrofuran (THF), and *N*,*N*′-dimethylformamide, followed by either acidic precipitation (*26*, *27*), hexane precipitation (*24*), dialysis (*28*), or atomization and drying (*29*). The use of organic solvents, such as ethylene glycol and THF, is an environmental concern and increases LNP cost for solvent recovery. In view of the facile production of LNPs directly from wood using *p*-TsOH fractionation, we fractionated the dissolved LNPs through centrifugation. We centrifuged the diluted spent liquor at 10 wt % at different speeds and then used AFM to examine the turbid supernatant. We found that large particles precipitated during centrifugation, whereas small particles remained in the supernatant. The supernatant from centrifugation at 3000*g* for 10 min contained lignin particle aggregates (Fig. 4C). Increasing the centrifuge speed to 10,000*g* or higher removed the aggregates and large particles, resulting in relatively uniform and small LNPs in the supernatant (Fig. 4, D and E). Typical LNP lateral sizes were approximately 200 and 50 nm at 10,000*g* and 15,000*g*, respectively. These results indicate that the precipitated LNPs can be fractionated by size using centrifugation. The AFM-measured height of the LNPs collected from centrifuging at 3000*g* and 10,000*g* had broad distributions (Fig. 4F), suggesting that

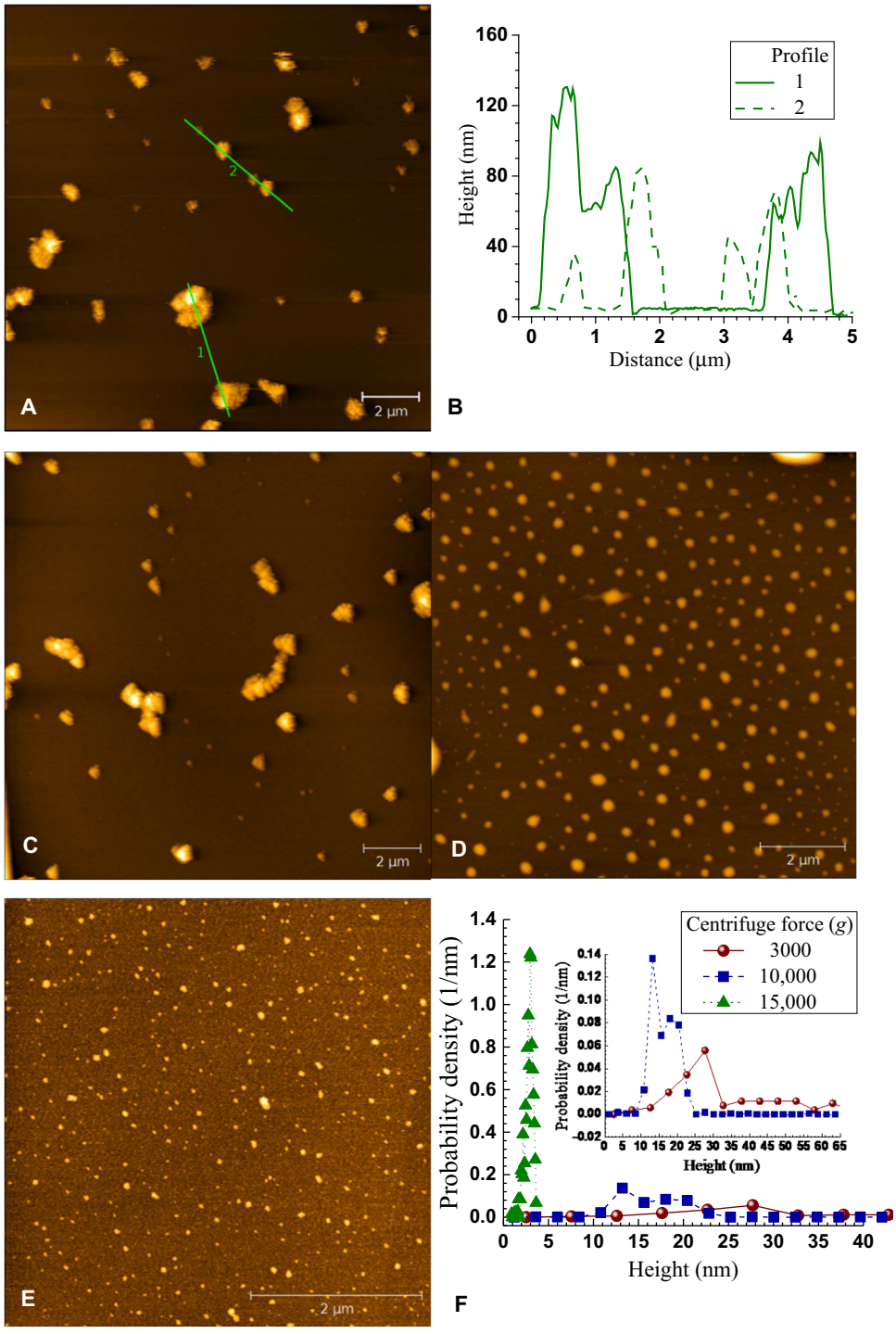

Fig. 4. Demonstration of centrifugation for fractionating solubilized LNPs. (**A**) AFM images of LNPs in a diluted spent *p*-TsOH liquor of 10 wt % that is produced using Wiley-milled NE222 at P75T80t20. (**B**) AFM-measured topographical height profiles corresponding to lines 1 and 2 in (A). (**C** to **E**) AFM images of LNPs in the supernatant from the centrifuged sample in (A) at different speeds for 10 min, at 3000*g* (C), at 10,000*g* (D), and at 15,000*g* (E). (**F**) AFM-measured topographical height distributions of samples shown in (C) to (E).

these particles are aggregated. However, the height distribution of the LNPs from centrifuging at 15,000*g* had a very sharp peak at approximately 3 nm, suggesting that these LNPs are primary and not aggregated particles. On the basis of the AFM-measured height of 3 nm (Fig. 4F) and lateral size of 50 nm in the images (Fig. 4E), we conclude that the primary nonaggregated LNPs were oblate spheroid nanoparticles with an aspect ratio (lateral or diameter to height or thickness) of approximately 20.

We found that fractionation condition affects LNP particle size and other properties. A more severe condition produced larger LNPs than

Table 2. Physical and chemical properties of the LNPs from dissolved lignin under three *p*-TsOH fractionation conditions.

Sample Abbreviation	DLS diameter (nm)	Zeta potential (mV)	Molecular weight		
			M_w	M_n	M_w/M_n
LNP-P70T50t20	349.7 ± 1.5	−40.0 ± 0.2	6900	2000	3.45
LNP-P70T65t20	371.7 ± 8.4	−36.5 ± 0.2	5800	2100	2.76
LNP-P75T80t20	467.1 ± 2.5	−37.9 ± 3.6	5400	2000	2.70

LNPs from a milder condition based on DLS measurements (Table 2). The three LNP samples shown in Table 2 represent delignification of approximately 85, 65, and 30% (Table 1), respectively, corresponding to DLS sizes of 467, 372, and 350 nm, respectively. Particle size increased substantially, from 372 to 467 nm, when delignification was increased from 65 to 85%, whereas particle size increased minimally, from 350 to 372 nm, when delignification was increased from 30 to 65%; this suggests that lignin condensation may have occurred at 85% lignin removal or under severe treatment conditions. The zeta potential of the LNPs decreased with the increase in particle size. Gel permeation chromatography (GPC) measurements indicated that the weight-average molecular weight (M_w) of LNPs decreased with the increase in fractionation severity (Table 2), whereas the number-average molecular weight (M_n) was mostly unchanged. M_w was 5400 under the most severe condition of P75T80t20 and increased to 6900 of P70T50t20. The polydispersity index (M_w/M_n) decreased with fractionation severity, indicating that a severe condition depolymerized lignin with homogeneous molecular weight. We saw a bimodal molecular weight distribution from all these fractionations (fig. S1).

Two-dimensional nuclear magnetic resonance spectroscopy of dissolved lignin fractions

We analyzed the dissolved lignin fractions from poplar under different treatment conditions (that is, P75T80t20, P70T65t20, and P70T50t20), along with the native lignin in poplar whole-cell walls (WCWs) using two-dimensional (2D) $^{1}H–^{13}C$ correlation nuclear magnetic resonance (NMR) spectroscopy. Figure 5 shows the four NMR spectra depicting the side-chain and aromatic regions, along with the identified chemical structures. Table 3 lists the $^{1}H–^{13}C$ contour integration data for the lignin structures. Native lignin and *O*-acetyl-β-D-glucuronoxylan structures are visible from the WCW spectrum. Native lignin in poplar contains predominantly syringyl β-aryl ether linkages (A-S) with a small amount of guaiacyl β-aryl ether linkages (A-G). The correlations for β-aryl ethers are shown for Aα [5.02/72.3 parts per million (ppm)], Aβ-S (4.24/86.3 ppm), and Aγ (3.73/60.3 ppm). A small amount of resinol linkages (C) were detected with correlations for Cα and Cβ at 4.72/85.1 and 3.08/54.1 ppm, respectively. Phenylcoumarans (normally abundant in softwood) were detected at a very low abundance in poplar and thus are not visible in the WCW spectrum at the intensity shown. The aromatic units in poplar (as with most hardwood species) are predominantly syringyl (S) with a small amount of guaiacyl (G). We estimated an S/G ratio of 3.4 (Table 3). Poplar also features *p*-hydroxybenzoates (PB), which are believed to exclusively acylate the γ-position of lignin side-chains, similar to *p*-coumarates in grasses (*30*). The PB (2/6) correlation is at 7.74/131.6 ppm. We estimated the quantity of PB at 14% of the total S (including syringyl α-ketones) and G units (Table 3). *O*-Acetyl-β-D-glucuronoxylan (Xyl) structures shown in the WCW are represented by the main chain correlations: β-D-Xyl*p*(1) (4.40/102.3 ppm), β-D-Xyl*p*(2) (3.22/73.1 ppm), β-D-Xyl*p*(3) (3.45/74.5 ppm), β-D-Xyl*p*(4) (3.65/75.7 ppm), and β-D-Xyl*p*(5) (3.31/63.3 and 3.99/63.3 ppm), along with the *O*-acetyl substituents (2-*O*-Ac-Xyl*p* and 3-*O*-Ac-Xyl*p*) at 4.66/73.6 and 4.95/75.0 ppm, respectively, 2,3-di-*O*-Ac-Xyl*p* at 4.75/71.3 ppm, and 4-*O*-methyl-α-D-glucuronic acid substituents (MeGlcA) at 5.33/97.7 ppm. We did not assign cellulose and other hemicelluloses in poplar WCW (gray contours) here because of unresolved contours.

The NMR spectrum of the lignin dissolved with severe treatment (P75T80t20) indicates that the sample is completely devoid of all polysaccharides and has significant structure changes in comparison to the WCW lignin. For example, the spectrum shows no β-aryl ether (Aα or Aβ) nor resinol (Cα, Cβ, or Cγ) contours; the Aγ contour (if present) would be within the unassigned contour at approximately 3.7/60 ppm. The contours of S and G units substantially shrank, probably caused by lignin condensation at the 2-, 5-, and 6-positions because any new aromatic linkages at these positions would lack hydrogens and would be consequently invisible in the $^{1}H–^{13}C$ correlation spectra. We suggest that the most severe treatment effectively depolymerized the lignin and also led to lignin condensation, consistent with the particle size measurements in Table 2 and the observation in Fig. 2D. A milder P70T65t20 treatment led to an efficient removal of the polysaccharides but minor impact on the lignin as compared to P75T80t20. For example, most of the native lignin structures (β-aryl ethers and resinols) remained intact. However, the NMR integration data (Table 3) indicated that some β-aryl ether linkages were cleaved, as evidenced by a decrease in the β-aryl ether fraction (that is, from 93 to 87%). Furthermore, the molecular weight data (Table 2) also indicated the partial cleavage of the β-aryl ether linkages because the M_w (5800) was significantly lower than that (usually >20,000) of native lignin (*31*). The increase in PB/(total lignin content) (that is, from 14 to 22%) indicated that the mild treatment depleted the lignin aromatics. Moreover, the slight increase in the S/G ratio (that is, from 1.8 to 2.3) indicated that the G units are preferentially degraded and subsequent condensation reactions have made the G units less visible in the NMR spectrum, as previously mentioned. The lignin dissolved with the mildest P70T50t20 treatment showed very similar NMR spectra to that of P70T65t20, with efficient removal of the polysaccharides and almost intact lignin structures. In addition, the integration data of P70T50t20 were similar to those of P70T65t20, with some minor differences in the PB/(total lignin content) and S/G ratio (Table 3).

From the NMR results, we suggest that lowering the *p*-TsOH concentration from 75 to 70 wt % and the temperature from 80° to 65°C still allows for the separation of lignin from the polysaccharides in the wood cell wall. Furthermore, lowering the treatment temperature from 65° to 50°C still allowed the effective dissolution and separation of lignin. We hypothesize that a certain degree of lignin cleavage is required to separate the polysaccharides, and the partial hydrolysis of lignin with these mild treatments demonstrates the intimate proximity lignin polymers have with matrix polysaccharides.

Enzymatic digestibility of WIS fraction

The substantial dissolution of lignin and hemicelluloses by *p*-TsOH resulted in good enzymatic digestibility of the fractionated NE222 WIS to produce sugars. We conducted enzymatic hydrolysis using a commercial cellulase (CTec3 of Novozymes) at a loading of 20 filter paper units (FPU)/g glucan in acetate buffer at elevated pH 5.5 that

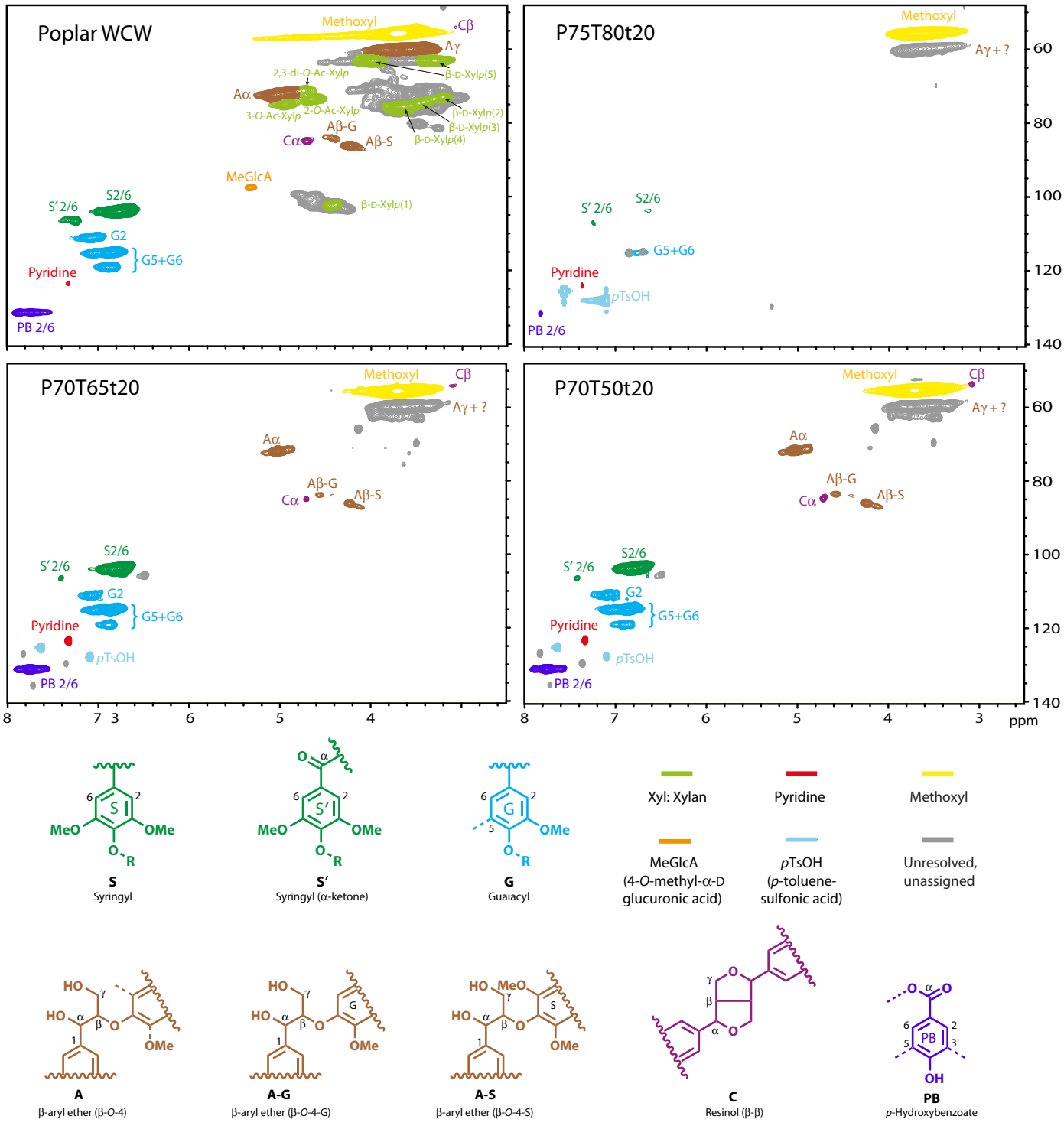

Fig. 5. Aromatic and side-chain (δC/δH 48–140/2.5–8.0) regions in the 2D HSQC NMR spectra of the WCW and three dissolved lignin samples from poplar wood.

led to reduced nonproductive cellulase binding to lignin (*32*, *33*). We achieved a solid substrate cellulose enzymatic digestibility (SED) of more than 90% (Fig. 6A) for the substrates produced at P75T65t35 and P75T65t60. Here, we define SED as the percentage of substrate glucan enzymatically saccharified into glucose. We also achieved an SED of more than 75% using a sample fractionated only for 5 min at 65°C (P75T65t05), indicating the efficiency of *p*-TsOH for wood fractionation. We suggest that a lower cellulase loading could be used to achieve reasonable glucose yield, as demonstrated using the substrate P75T80t20 (Fig. 6B).

Table 3. Structural characteristics (lignin interunit linkages, PB, aromatic units, and S/G ratio) from integration of $^{1}H–^{13}C$ correlation peaks in the HSQC spectra of the WCW and three dissolved lignins from poplar wood. Numbers for Lignin Interunit linkages are percent of the sum of the integrals for structures Aa and Ca is accounted for by the integral for each individual structure. Numbers for PB2/6 are percentage of total lignin content (G + S + S′) in each sample spectrum.

	WCW	P75T80t20	P70T65t20	P70T50t20
Lignin interunit linkages				
β-*O*-4 aryl ethers (A)	93	—	87	87
Resinols (C)	7	—	13	13
p-Hydroxybenzoates ($PB_{2/6}$)	14	—	22	20
Lignin aromatic units				
G (%)	36	—	30	34
S (%)	64	—	70	66
S/G ratio	1.8	—	2.3	1.9

Mechanisms of carbohydrates and lignin dissolution by *p*-TsOH

As a strong organic acid (pK_a = −2.8 at 20°C), *p*-TsOH can easily donate a proton in an aqueous solution to catalyze hydrolysis or reactions to break glycosidic, ether, and ester bonds in carbohydrates, lignins, and lignin-carbohydrate complexes (fig. S2). As a result, hydrolysis of hemicelluloses by *p*-TsOH can release xylose and mannose. Glucose can also be released from some easily hydrolyzable cellulose. The measured monomeric sugar concentrations in the spent acid liquor (Table 1) show this.

Because of variations in hydrotrope structures, the exact mechanism of a given hydrotrope solubilizing compounds is still under debate (*18*). However, most researchers believe that most hydrotropes aggregate above the MHC (*18*, *19*). Aggregation is pronounced in the presence of a hydrophobic solute (*34*). We can therefore hypothesize that the solubilization of lignin that is highly hydrophobic in aqueous *p*-TsOH above the MHC of approximately 11.5 wt % is a result of this aggregation. In general, the separated lignin undergoes intermolecular condensation, or recondensation, to be redeposited onto a solid substrate in the absence of strong hydrophilic nucleophilic agents in an acidic environment. However, we observed no precipitates after centrifugation when the *p*-TsOH concentration in the spent acid liquor was above the MHC. We further hypothesize that the lipophilic nonpolar part (toluene moiety) of the *p*-TsOH molecule can shield the separated lignin through the π-π stacking or hydrophobic interaction to form micellar-like aggregates to prevent the reaggregation of lignin, whereas the hydrophilic end (sulfonic acid moiety) points outward to water for effective dissolution (Fig. 1B) (*19*).

When the spent *p*-TsOH liquor is diluted with water to below the MHC, *p*-TsOH loses its hydrotropy, which destabilizes aggregation, resulting in lignin precipitation. We hypothesize that the precipitated lignin particles could couple or entrap *p*-TsOH molecules to become charged, owing to the dissociation of the entrapped *p*-TsOH, along with the functional groups on lignin. After the removal of excess acid by centrifuging and washing, the charged LNPs can disperse in water because of the electrostatic repulsion (Figs. 1B and 4, D and E).

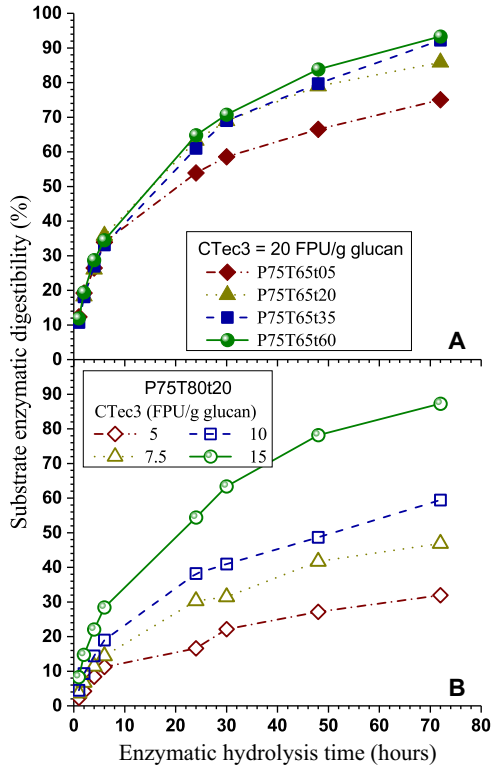

Fig. 6. Time-dependent enzymatic digestibility of fractionated NE222 WISs. (**A**) Different substrates from various fractionation conditions under constant cellulase loading of CTec3 = 20 FPU/g glucan. (**B**) Effects of cellulase CTec3 loading.

p-TsOH recyclability and potential hemicellulosic sugar recovery

We conducted a preliminary evaluation of the reusability of *p*-TsOH by fractionating Wiley-milled poplar NE222 under two conditions (table S1). We first removed the WIS through filtration after the first-cycle fractionation for each reaction condition conducted. We calculated the amount of fresh makeup *p*-TsOH solution needed for the second cycle on the basis of the volume of the collected spent acid liquor with the assumption that *p*-TsOH consumption by reaction was negligible. We then added the predetermined amount of fresh makeup *p*-TsOH solution to the collected spent liquor along with the same amount of fresh poplar after heating the liquor to the desired reaction temperature. We compared the chemical compositions from the first and second cycles (table S2). The differences were within measurement error, suggesting good recyclability and reusability (reactivity) of *p*-TsOH. We need further studies to quantify *p*-TsOH recovery with more cycles.

Because of the rapid and low-temperature (≤80°C) fractionation, no further degradation of the dissolved hemicellulosic sugars in the spent *p*-TsOH liquor occurred (Table 1), even after several times of reusing the liquor without dilution to precipitate lignin. The lignin and hemicellulosic sugars accumulated to result in a concentrated stream. By diluting the spent liquor to 5 to 10 wt % and separating the dissolved lignin, the dissolved hemicellulosic sugars can be recovered in the form of furfural through catalysis using the *p*-TsOH in the diluted liquor stream as catalyst at elevated temperatures of approximately 130°C (Fig. 1A), as we demonstrated previously (*35*) using corn cob with a good yield. We may use membrane filtration for effective separation in future studies.

CONCLUSIONS

We demonstrated that hydrotropic *p*-TsOH can achieve near-complete solubilization of wood lignin at low temperatures of ≤80°C for approximately 20 min. We separated the dissolved lignin by diluting the spent acid liquor below the MHC of 11.5 wt %. We efficiently fractionated poplar wood to produce sugars through the enzymatic saccharification of the cellulose-rich WIS fraction and LNPs from the dissolved lignin fraction. We used 2D NMR spectroscopy to further confirm the efficient separation of lignin from polysaccharides from poplar wood under mild conditions while leaving a substantial portion of lignin structurally intact, which could be tailored for lignin valorization. We suggest converting the dissolved hemicellulosic sugars to furfural after lignin precipitation. We found that the used *p*-TsOH, as a catalyst and solvent, did not lose its hydrotrope activity and can be reused with excellent activity. Because of its low solubility in water at ambient temperatures, we can therefore efficiently recover *p*-TsOH using commercial crystallization technology by cooling the reconcentrated diluted spent liquor after lignin precipitation. The acid hydrotrope chemistry presented here has broad applications for low-cost fractionation of a variety of lignocelluloses, especially nonwoody plant biomass for sustainable economic development through biorefining.

MATERIALS AND METHODS

Materials

We obtained logs of poplar NE222 (*Populus deltoides* Bartr. ex Marsh. × *P. nigra* L.) from R. Zalesny Jr. [Northern Research Station, U.S. Department of Agriculture (USDA) Forest Service], who harvested from the Hugo Sauer Nursery in Rhinelander, WI. We manually debarked the logs and chipped them at the Forest Products Laboratory, USDA Forest Service. We ground the wood chips into a 20-mesh powder using a Wiley mill (model no. 2, Arthur H. Thomas Co.). We purchased the *p*-TsOH from Sigma-Aldrich and received commercial cellulase (CTec3) complimentarily provided by Novozymes.

Fractionation using *p*-TsOH

We prepared the *p*-TsOH solutions of desired mass concentrations by adding the required amounts of *p*-TsOH and DI water into a 150-ml flask. We then heated 50 ml of acid solution in the flask to a desired temperature, followed by the addition of 5 g (oven-dry weight) of Wiley-milled NE222 powders. We conducted fractionation reactions on a shaker (Excella 25, Eppendorf) at 200 rpm for 5 to 60 min at various acid concentrations between 70 and 85 wt % and temperatures between 50° and 80°C. At the end of the preset reaction time, we added an appropriate amount of cold water into the flask to dilute the acid concentration and terminate the reaction. We separated the solids from the spent liquor using vacuum filtration. We collected the filtrate to produce LNPs. We thoroughly washed the solids using DI water until neutral pH was reached. We analyzed the chemical composition of the resulting washed WISs.

Composition analysis

We dried small samples of fractionated NE222 solids in an oven at 105°C overnight and then Wiley-milled the dried sample to 20-mesh powder after cooling down. We hydrolyzed the Wiley-milled untreated NE222 powder and the fractionated solids using sulfuric acid in two steps and then analyzed for carbohydrates and Klason lignin through the Analytical Chemistry and Microscopy Laboratory at the Forest Products Laboratory, as described previously (*36*).

AFM imaging

We used AFM imaging (AFM Workshop) to examine the LNP morphologies. We deposited a drop of diluted LNP suspension at approximately 0.1 g/liter onto a clean mica surface and air-dried the sample overnight in an ambient environment before imaging. We determined the heights of LNPs using the Gwyddion imaging analysis software (Department of Nanometrol, Czech Metrology Institute) equipped with the AFM system.

Particle sizing by DLS

We measured the DLS size of LNPs using a zeta potential analyzer (NanoBrook Omni, Brookhaven Instruments). We circulated the samples five times for a total of 10 min to obtain the averaged size for each sample.

Lignin molecular weight determination using GPC

We dissolved 0.1 g of the freeze-dried lignin sample from the turbid LNP suspension in 2 ml of pyridine-acetic anhydride (1:1 by volume) solution. We kept the solution in a dark cabinet for 3 days at room temperature. We then added the solution dropwise into 120 ml of ice-cold diluted HCl solution of 0.08% volumetric concentration with constant stirring. We filtrated the solution using a 10-μm nylon membrane and collected the precipitated lignin acetate, washed it with water, and then dried it in air and under vacuum at 50°C. We used GPC to estimate the M_n and M_w of the acetylated lignin samples on an ICS-3000 system (Dionex) with three 300 × 7.8–mm [length × inner diameter (l. × i.d.)] Phenogel 5U columns (10,000, 500, and 50 Å) and a 50 × 7.8–mm (l. × i.d.) Phenogel 5U guard column (Phenomenex) (*37*). We dissolved 5 mg of lignin acetate in 1 ml of high-performance liquid chromatography–grade THF without a stabilizer and injected 50 μl of the resulting solution into the GPC columns at 30°C, with THF as eluent at a flow rate of 1 ml/min. We used polystyrene standards for calibration and a variable wavelength detector at 280 and 254 nm, respectively, to detect lignin and polystyrene, respectively.

NMR sample preparation and analyses

WCW preparation

We ball-milled the poplar wood sample for 2 min at 30 Hz using a Retsch MM 400 mixer mill with corrosion-resistant stainless steel screw-top grinding jars (50 ml) containing a single steel ball (30 mm). We first extracted the WCW powder from the ball-milled poplar using distilled water (three times), 80% ethanol (three times), and then acetone (three times) consecutively using ultrasonication (Branson 3510R-MT, Branson Ultrasonics Corporation). Finally, we finely milled the extractive-free isolated cell walls using a Fritsch Pulverisette 7 planetary ball mill spinning at 600 rpm with zirconium dioxide (ZrO_2) vessels (50 ml) containing ZrO_2 balls (10 mm × 10 mm). The grinding time for all three samples was 23 cycles (each cycle contains a 10-min interval with a 5-min interval break).

NMR spectroscopy for WCW and dissolved lignin

We performed the solution-state NMR experiments in dimethyl sulfoxide (DMSO)–d_6–pyridine–d_5 (*38*) at 27°C on a Bruker AVANCE III spectrometer operating at 400.13 and 100.61 MHz for ^{1}H and ^{13}C, respectively. We processed the NMR data using the TopSpin 3.0 software. We denoted chemical shifts (δ) in parts per million and coupling constants (*J* values) in hertz. We used the central DMSO-pyridine solvent peak as internal reference (δ ^{13}C, 39.5 ppm; δ ^{1}H, 2.49 ppm). We acquired phase-sensitive 2D ^{1}H–^{13}C heteronuclear single-quantum coherence (HSQC) spectra with spectral widths of 12 ppm for ^{1}H and 220 ppm for ^{13}C using a 2-s relaxation delay, 1K data points, 256 t_1 increments, and 64 transients. We used an adiabatic version of the HSQC experiment

(hsqcetgpsisp.2 pulse sequence from the Bruker Library). We colored the spectral images using Adobe Illustrator CS6 and created the chemical structures using ChemDraw Pro 14.0.

SUPPLEMENTARY MATERIALS

Supplementary material for this article is available at http://advances.sciencemag.org/cgi/content/full/3/9/e1701735/DC1

fig. S1. Optical microscopy images of wood fibers produced using *p*-TsOH fractionation under low-severity conditions (fiber lignin content, 16%), followed by mechanical refining to 550-ml Canadian Standard Freeness.

fig. S2. GPC-measured molecular weight distribution of LNPs from fractionation of Wiley-milled poplar NE222 using *p*-TsOH under three different conditions.

fig. S3. Catalysis of carbohydrate hydrolysis and lignin degradation by *p*-TsOH.

table S1. Duplicate fractionation runs under six sets of conditions to demonstrate the repeatability of *p*-TsOH fractionation experiments.

table S2. Comparisons of chemical compositions of fractionated poplar NE222 WISs between the first cycle using fresh *p*-TsOH solution and the recycle run using spent *p*-TsOH acid liquor.

REFERENCES AND NOTES

1. A. J. Ragauskas, C. K. Williams, B. H. Davison, G. Britovsek, J. Cairney, C. A. Eckert, W. J. Frederick Jr., J. P. Hallett, D. J. Leak, C. L. Liotta, J. R. Mielenz, R. Murphy, R. Templer, T. Tschaplinski, The path forward for biofuels and biomaterials. *Science* **311**, 484–489 (2006).
2. S. Tian, W. Zhu, R. Gleisner, X. J. Pan, J. Y. Zhu, Comparisons of SPORL and dilute acid pretreatments for sugar and ethanol productions from aspen. *Biotechnol. Prog.* **27**, 419–427 (2011).
3. Y. L. Zhao, Y. Wang, J. Y. Zhu, A. Ragauskas, Y. L. Deng, Enhanced enzymatic hydrolysis of spruce by alkaline pretreatment at low temperature. *Biotechnol. Bioeng.* **99**, 1320–1328 (2008).
4. X. J. Pan, C. Arato, N. Gilkes, D. Gregg, W. Mabee, K. Pye, Z. Z. Xiao, X. Zhang, J. Saddler, Biorefining of softwoods using ethanol organosolv pulping: Preliminary evaluation of process streams for manufacture of fuel-grade ethanol and co-products. *Biotechnol. Bioeng.* **90**, 473–481 (2005).
5. M. Iakovlev, A. van Heiningen, Efficient fractionation of spruce by SO_2-ethanol-water treatment: Closed mass balances for carbohydrates and sulfur. *ChemSusChem* **5**, 1625–1637 (2012).
6. J. S. Luterbacher, J. M. Rand, D. M. Alonso, J. Han, J. T. Youngquist, C. T. Maravelias, B. F. Pfleger, J. A. Dumesic, Nonenzymatic sugar production from biomass using biomass-derived γ-valerolactone. *Science* **343**, 277–280 (2014).
7. A. Brandt, M. J. Ray, T. Q. To, D. J. Leak, R. J. Murphy, T. Welton, Ionic liquid pretreatment of lignocellulosic biomass with ionic liquid–water mixtures. *Green Chem.* **13**, 2489–2499 (2011).
8. J. Y. Zhu, X. J. Pan, G. S. Wang, R. Gleisner, Sulfite pretreatment (SPORL) for robust enzymatic saccharification of spruce and red pine. *Bioresour. Technol.* **100**, 2411–2418 (2009).
9. J. Y. Zhu, M. S. Chandra, F. Gu, R. Gleisner, R. Reiner, J. Sessions, G. Marrs, J. Gao, D. Anderson, Using sulfite chemistry for robust bioconversion of Douglas-fir forest residue to bioethanol at high titer and lignosulfonate: A pilot-scale evaluation. *Bioresour. Technol.* **179**, 390–397 (2015).
10. A. Ferrer, E. Quintana, I. Filpponen, I. Solala, T. Vidal, A. Rodríguez, J. Laine, O. J. Rojas, Effect of residual lignin and heteropolysaccharides in nanofibrillar cellulose and nanopaper from wood fibers. *Cellul.* **19**, 2179–2193 (2012).
11. A. Rahimi, A. Ulbrich, J. J. Coon, S. S. Stahl, Formic-acid-induced depolymerization of oxidized lignin to aromatics. *Nature* **515**, 249–252 (2014).
12. L. Shuai, M. T. Amiri, Y. M. Questell-Santiago, F. Héroguel, Y. Li, H. Kim, R. Meilan, C. Chapple, J. Ralph, J. S. Luterbacher, Formaldehyde stabilization facilitates lignin monomer production during biomass depolymerization. *Science* **354**, 329–333 (2016).
13. D. M. Alonso, S. H. Hakim, S. Zhou, W. Won, O. Hosseinaei, J. Tao, V. Garcia-Negron, A. H. Motagamwala, M. A. Mellmer, K. Huang, C. J. Houtman, N. Labbé, D. P. Harper, C. Maravelias, T. Runge, J. A. Dumesic, Increasing the revenue from lignocellulosic biomass: Maximizing feedstock utilization. *Sci. Adv.* **3**, e1603301 (2017).
14. A. R. Procter, A review of hydrotropic pulping. *Pulp Paper Mag. Can.* **72**, 67–74 (1971).
15. K. Gabov, R. J. A. Gosselink, A. I. Smeds, P. Fardim, Characterization of lignin extracted from birch wood by a modified hydrotropic process. *J. Agric. Food Chem.* **62**, 10759–10767 (2014).
16. Y.-H. P. Zhang, S.-Y. Ding, J. R. Mielenz, J.-B. Cui, R. T. Elander, M. Laser, M. E. Himmel, J. R. McMillan, L. R. Lynd, Fractionating recalcitrant lignocellulose at modest reaction conditions. *Biotechnol. Bioeng.* **97**, 214–223 (2007).
17. H. Bian, L. Chen, R. Gleisner, H. Dai, J. Y. Zhu, Producing wood-based nanomaterials by rapid fractionation of wood at 80°C using a recyclable acid hydrotrope. *Green Chem.* **19**, 3370–3379 (2017).
18. J. Eastoe, M. H. Hatzopoulos, P. J. Dowding, Action of hydrotropes and alkyl-hydrotropes. *Soft Matter* **7**, 5917–5925 (2011).
19. S. Das, S. Paul, Mechanism of hydrotropic action of hydrotrope sodium cumene sulfonate on the solubility of di-t-butyl-methane: A molecular dynamics simulation study. *J. Phys. Chem. B* **120**, 173–183 (2016).
20. M. H. Hatzopoulos, J. Eastoe, P. J. Dowding, S. E. Rogers, R. Heenan, R. Dyer, Are hydrotropes distinct from surfactants? *Langmuir* **27**, 12346–12353 (2011).
21. A. P. Richter, J. S. Brown, B. Bharti, A. Wang, S. Gangwal, K. Houck, E. A. Cohen Hubal, V. N. Paunov, S. D. Stoyanov, O. D. Velev, An environmentally benign antimicrobial nanoparticle based on a silver-infused lignin core. *Nat. Nanotechnol.* **10**, 817–823 (2015).
22. E. Ten, C. Ling, Y. Wang, A. Srivastava, L. A. Dempere, W. Vermerris, Lignin nanotubes as vehicles for gene delivery into human cells. *Biomacromolecules* **15**, 327–338 (2014).
23. C. Jiang, H. He, H. Jiang, L. Ma, D. M. Jia, Nano-lignin filled natural rubber composites: Preparation and characterization. *Express Polym. Lett.* **7**, 480–493 (2013).
24. Y. Qian, Q. Zhang, X. Qiu, S. Zhu, CO_2-responsive diethylaminoethyl-modified lignin nanoparticles and their application as surfactants for CO_2/N-$_2$-switchable Pickering emulsions. *Green Chem.* **16**, 4963–4968 (2014).
25. S. S. Nair, S. Sharma, Y. Pu, Q. Sun, S. Pan, J. Y. Zhu, Y. Deng, A. J. Ragauskas, High shear homogenization of lignin to nanolignin and thermal stability of nanolignin-polyvinyl alcohol blends. *ChemSusChem* **7**, 3513–3520 (2014).
26. C. Frangville, M. Rutkevicius, A. P. Richter, O. D. Velev, S. D. Stoyanov, V. N. Paunov, Fabrication of environmentally biodegradable lignin nanoparticles. *Chemphyschem* **13**, 4235–4243 (2012).
27. A. P. Richter, B. Bharti, H. B. Armstrong, J. S. Brown, D. Plemmons, V. N. Paunov, S. D. Stoyanov, O. D. Velev, Synthesis and characterization of biodegradable lignin nanoparticles with tunable surface properties. *Langmuir* **32**, 6468–6477 (2016).
28. M. Lievonen, J. J. Valle-Delgado, M.-L. Mattinen, E.-L. Hult, K. Lintinen, M. A. Kostiainen, A. Paananen, G. R. Szilvay, H. Setälä, M. Österberg, A simple process for lignin nanoparticle preparation. *Green Chem.* **18**, 1416–1422 (2016).
29. M. Ago, S. Huan, M. Borghei, J. Raula, E. I. Kauppinen, O. J. Rojas, High-throughput synthesis of lignin particles (~30 nm to ~2 μm) via aerosol flow reactor: Size fractionation and utilization in pickering emulsions. *ACS Appl. Mater. Interfaces* **8**, 23302–23310 (2016).
30. J. Ralph, F. Lu, The DFRC method for lignin analysis. 6. A simple modification for identifying natural acetates on lignins. *J. Agric. Food Chem.* **46**, 4616–4619 (1998).
31. A. Tolbert, H. Akinosho, R. Khunsupat, A. K. Naskar, A. J. Ragauskas, Characterization and analysis of the molecular weight of lignin for biorefining studies. *Biofuel. Bioprod. Bior.* **8**, 836–856 (2014).
32. H. Lou, J. Y. Zhu, T. Q. Lan, H. Lai, X. Qiu, pH-induced lignin surface modification to reduce nonspecific cellulase binding and enhance enzymatic saccharification of lignocelluloses. *ChemSusChem* **6**, 919–927 (2013).
33. T. Q. Lan, H. Lou, J. Y. Zhu, Enzymatic saccharification of lignocelluloses should be conducted at elevated pH 5.2–6.2. *Bioenerg. Res.* **6**, 476–485 (2013).
34. W. Kunz, K. Holmberg, T. Zemb, Hydrotropes. *Curr. Opin. Colloid Interface Sci.* **22**, 99–107 (2016).
35. H. Ji, L. Chen, J. Y. Zhu, R. Gleisner, X. Zhang, Reaction kinetics based optimization of furfural production from corncob using a fully recyclable solid acid. *Ind. Eng. Chem. Res.* **55**, 11253–11259 (2016).
36. X. Luo, R. Gleisner, S. Tian, J. Negron, E. Horn, X. J. Pan, J. Y. Zhu, Evaluation of mountain beetle infested lodgepole pine for cellulosic ethanol production by sulfite pretreatment to overcome recalcitrance of lignocellulose. *Ind. Eng. Chem. Res.* **49**, 8258–8266 (2010).
37. X. Yang, N. Li, X. Lin, X. Pan, Y. Zhou, Selective cleavage of the aryl ether bonds in lignin for depolymerization by acidic lithium bromide molten salt hydrate under mild conditions. *J. Agric. Food Chem.* **64**, 8379–8387 (2016).
38. H. Kim, J. Ralph, Solution-state 2D NMR of ball-milled plant cell wall gels in DMSO-d_6/pyridine-d_5. *Org. Biomol. Chem.* **8**, 576–591 (2010).

Acknowledgments

Funding: This work was conducted while L.C., H.B., Q.M., and J.D. were visiting Ph.D. students and R.W. was a visiting a scholar at the Forest Products Laboratory (FPL), U.S. Department of Agriculture (USDA) Forest Service, and on official government time of J.Z. and D.J.Y. We acknowledge J. Ralph for his scientific advice and for letting us use his laboratory facilities at the U.S. Department of Energy Great Lakes Bioenergy Research Center, the University of Wisconsin-Madison for the WCW sample preparation, the NMR facilities and J. J. Koivisto from Aalto University School of Chemical Engineering for the technical support, and F. Matt at FPL for the compositional analysis. This work was partially supported by the USDA Agriculture and Food Research Initiative competitive grant (no. 2011-67009-20056), the Guangzhou Elite Project of China, the Chinese State Forestry Administration (project no. 2015-4-54), the Doctorate Fellowship Foundation of Nanjing Forestry University, the Finnish Cultural Foundation, the Chinese Scholarship Council (CSC), and the Guangxi Scholarship

Fund. Funding from these programs made the visiting appointments of L.C., H.B., J.D., Q.M., and R.W. at FPL possible. N.L. and X.P. also acknowledge the financial support from the USDA McIntire Stennis Fund (WIS01861) and the CSC for N.L.'s doctoral program at the University of Wisconsin-Madison. **Author contributions:** All authors contributed to the data analyses and manuscript writing. J.Z. initiated the concept of low-temperature wood fractionation using *p*-TsOH, designed the initial fractionation conditions, and conducted most of the data analyses and writing. L.C. and J.Z. conducted most of the fractionation experiments and, along with S.F., designed the experiments for LNP separation, AFM imaging, and carbohydrate analyses of the solids and liquor stream. J.D., D.J.Y., and T.V. designed and conducted the dissolved lignin NMR experiments and analyses. N.L. and X.P. conducted the dissolved lignin molecular weight measurements using GPC. R.W., along with L.C., conducted the enzymatic hydrolysis of fractionated solids and sugar analyses. Q.M., H.B., and J.Z., along with L.C., conducted the additional fractionation experiments and *p*-TsOH recycling and reusability study. **Competing interests:** J.Z. and L.C. are co-inventors on a patent application related to this work filed by FPL (U.S. Provisional Patent application no. 62/452,282, filed 01 January 2017). All other authors declare that they have no competing interests. **Data and materials availability:** All data needed to evaluate the conclusions in the paper are present in the paper and/or the Supplementary Materials. Additional data related to this paper may be requested from the authors.

Submitted 24 May 2017
Accepted 16 August 2017
Published 15 September 2017
10.1126/sciadv.1701735

Citation: L. Chen, J. Dou, Q. Ma, N. Li, R. Wu, H. Bian, D. J. Yelle, T. Vuorinen, S. Fu, X. Pan, J. (J.Y.) Zhu, Rapid and near-complete dissolution of wood lignin at ≤80°C by a recyclable acid hydrotrope. *Sci. Adv.* **3**, e1701735 (2017).

Science Advances

Rapid and near-complete dissolution of wood lignin at ≤80°C by a recyclable acid hydrotrope

Liheng Chen, Jinze Dou, Qianli Ma, Ning Li, Ruchun Wu, Huiyang Bian, Daniel J. Yelle, Tapani Vuorinen, Shiyu Fu, Xuejun Pan and Junyong (J.Y.) Zhu

Sci Adv **3** (9), e1701735.
DOI: 10.1126/sciadv.1701735